DTU Library

Towards a regional wind farm planning approach: The Wakeness Index

Alonso-De-Linaje, Nicolas Gonzalez; Hahmann, Andrea N.; Peña, Alfredo

Published in:
Proceedings of Wake Conference 2025 10/06/2025 - 12/06/2025 Visby, Sweden

Link to article, DOI:
10.1088/1742-6596/3016/1/012050

Publication date:
2025

Document Version
Publisher's PDF, also known as Version of record

Journal of Physics:
Conference Series

PAPER • OPEN ACCESS

Towards a regional wind farm planning approach: The Wakeness Index

To cite this article: Nicolas Gonzalez Alonso-De-Linaje *et al* 2025 *J. Phys.: Conf. Ser.* **3016** 012050

Journal of Physics: Conference Series **3016** (2025) 012050 doi:10.1088/1742-6596/3016/1/012050

Towards a regional wind farm planning approach: The Wakeness Index

Nicolas Gonzalez Alonso-de-Linaje[1], **Andrea N. Hahmann**[1] **and Alfredo Peña**[1]

[1]Department of Wind and Energy Systems, Technical University of Denmark (DTU), Roskilde, Denmark

E-mail: nicdel@dtu.dk

Abstract. Offshore wind energy expansion often involves large wind farms built in close proximity, where inter-farm wake interactions can significantly impact energy production. Numerical weather prediction (NWP) models such as the Weather Research and Forecasting (WRF) model can capture these interactions but are computationally expensive for exploring multiple future scenarios. To address this limitation, we introduce the Wakeness Index (WIX), a simplified yet scalable tool for preliminary regional wind farm planning. Two variants of the WIX are presented: $\mathrm{WIX_G}$, which captures basic geometric interactions among wind turbines, and $\mathrm{WIX_C}$, which incorporates local wind climatology to improve accuracy. Both variants show strong agreement with WRF-based wind speed deficit results, with correlations of up to 0.93, yet require a fraction of the computational resources and time. Although $\mathrm{WIX_C}$ offers higher fidelity, it runs at a rate roughly twenty-eight times slower than $\mathrm{WIX_G}$, underscoring the trade-off between speed and complexity. This study highlights the applicability of the WIX for rapid scenario assessments, enabling stakeholders to identify optimal spatial layouts for offshore wind farms before engaging into more detailed, resource-intensive simulations. The WIX streamlines the planning process for large-scale offshore wind projects, facilitating sustainable development and efficient utilization of marine space.

1 Introduction

Offshore wind energy development has accelerated rapidly, particularly in the North Sea, to meet growing energy demands [1] and mitigate climate change. As a result, ever larger wind farms are being built close together, intensifying inter-farm interactions. These interactions can adversely affect the efficiency of wind energy production because the wakes of one farm may overlap with neighboring sites, reducing performance [16, 2]. Studying the potential wake effects from wind farms is critical to maximizing energy yield and optimizing the spatial planning in a region. However, numerical methods for regional wake modeling are computationally expensive and scenario-dependent, making the efficient assessment of multiple wind farm configurations challenging.

Regional wind farm wake modeling is typically carried out with wind farm parameterizations implemented in numerical weather prediction (NWP) models such as the Weather Research and Forecasting (WRF) model. Two well-known wind farm parameterizations are the explicit wind farm parameterization (EWP) and the wind farm parameterization (Fitch) ([16, 9]). However, the studies using these parameterizations might not be accurate even at the resolution of these models [11, 14]. Moreover, the heavy computational requirements of these models reduce the ability of stakeholders to investigate multiple future scenarios, an essential step in planning sustainable offshore wind energy expansions. To address this challenge in a more streamlined manner, we propose the "wakeness" index (WIX) for preliminary wind farm planning assessments. The WIX uses basic wind farm configuration geometry and wind field statistics to provide an affordable and scalable way of assessing wake impacts at regional scales. This index provides guidance on the expectation of wakes over an area that is being scrutinized for possible wind harvesting. Higher WIX values indicate a greater chance of wakes impacting the investigated area.

Despite the WIX being an indicator and not a wake model, it allows users to explore scenarios before using high-fidelity tools, providing guidance about where and how to use modeling frameworks such as regional climate models, large eddy simulations, or engineering wake models used in the industry. From a planning perspective, quantifying the spatial influence of wind farm wakes is crucial for integrated regional development. Offshore spaces are busy with diverse activities, e.g., fishing, navigation, and the habitat of marine species, which makes it vital to account for how new or expanding wind farms might interact with these uses. The WIX can rapidly deliver wind farm footprints across key spatial components, such as protected areas, shipping lanes, and critical ecosystems, by focusing on geometry-based interactions and mean wind statistics. This enables stakeholders to compare multiple layouts and identify optimal strategies for expanding offshore wind without compromising other marine interests.

This work outlines how the WIX works and how it can be applied to preliminary wind farm scenario planning. First, we introduce the current wind energy scenario in the North Sea and the incoming challenges. Then, we illustrate how the WIX methodology addresses computational bottlenecks, facilitating the quick assessment of numerous wind farm scenarios. Finally, we address how to apply this methodology to real cases.

2 Data

2.1 Wind farm dataset for 2030 future scenario

We use the wind farm layouts of a possible scenario for future wind farm deployment in 2030 (Y2030). The database for the current deployments combines information from national datasets [3, 6, 5], a European-wide wind farm database [15], OpenStreetMap [13] and the European Marine Observation and Data Network (EMODnet) [7]. Besides the location of the wind turbines, the database also contains the turbine type, hub height and rotor diameter, rated power, cut-in and cut-out wind speed and the turbine power and thrust curve. The Y2030 scenario consists of a dataset of polygons and installed capacities of the locations of future offshore wind farms [6]. The polygon provides the boundary of the area and a target installed capacity.

We fill the polygons with the IEA 15 MW ([10]) turbine using a clustering algorithm to maximize the distance among the wind turbines. The algorithm is based on K-means clustering, where the computed wind farm's total number of wind turbines sets the number of targeted clusters. Finally, the centroid of every cluster gives the wind turbine position $wt_{i,j}$ when the iteration process converges. The K-means algorithm aims to choose centroids that minimize the within-cluster sum-of-squares criterion, as follows:

$$wt_{i,j} = \sum_{i=0}^{n} \min_{\mu_j \in C}(\|x_i - \mu_j\|^2) \tag{1}$$

where μ_j is the cluster centroid and x_i is every point within the cluster C.

2.2 Wind field climatology

The climatological statistics of the wind field come from the New European Wind Atlas (NEWA) [4] in its microscale form. This dataset uses a detailed modeling approach to depict wind climatologies across Europe. For microscale analysis, NEWA employs the Wind Atlas Analysis and Application Program (WAsP) to refine mesoscale simulations, capturing detailed wind variations affected by local terrain features.

2.3 The WRF model runs for the 2030 scenario

The 2030 scenario simulations were conducted using the WRF model in two configurations: one with the EWP wind farm parameterization [16] enabled ($\mathrm{WRF_{EWP}}$), and one without any wind farm parameterization ($\mathrm{WRF_{NOWF}}$). All simulations are run for a single "representative" calendar year. To ensure that the selected year reflects typical wind energy conditions, a representative year analysis was performed following the approach described in [8]. In this context, a "typical year" is defined as one that closely matches the long-term climatological distributions of wind speed, wind direction, and atmospheric stability. Based on this analysis, the year 2019 was selected. The simulation domain encompasses the entire North Sea and parts of the Baltic Sea.

Here, the quantity extracted from the WRF output is the yearly-averaged wind speed deficit ($\mathrm{WRF_{deficit}}$), which is the absolute difference between $\mathrm{WRF_{NOWF}}$ and $\mathrm{WRF_{EWP}}$ at 100 m amsl. Moreover, for some comparison cases, the $\mathrm{WRF_{deficit}}$ was normalized by its minimum and maximum so it was non-dimensional as the WIX.

3 Methods

3.1 The wakeness index

The WIX assesses wake impacts on a regional scale using wind farm geometry and wind field statistics. It aims to test multiple scenarios to predict wake effects in areas considered for wind energy harvesting, with higher values indicating a greater likelihood of wake influence. Two versions of the WIX are proposed: a geometry-only index ($\mathrm{WIX_G}$), which only takes as input the wind farm geometries, and a climatology-based index ($\mathrm{WIX_C}$), which is the $\mathrm{WIX_G}$ weighted by the wind direction frequencies from the climatology at the wind farm location. Despite the two variants, the WIX is calculated at every possible turbine position at all the wind direction sectors. The method starts by setting directional rays R defined as

$$R = \sqrt{(wt_x + r\sin\phi)^2 + (wt_y + r\cos\phi)^2}, \tag{2}$$

where ϕ is the wind direction at every possible turbine position $wt_{x,y}$, propagating into all directions with radial steps of 5° for a given distance r =100 km, which is defined based on extreme wake statistics on the study region ([12]). Moreover, a decay kernel N_d based on a Gaussian distribution is applied to account for the wake decay effect (see Figure 1-left panel)

$$N_d = \frac{1}{\sqrt{2\pi\sigma^2}}\exp\left(-\frac{(d-\mu)^2}{2\sigma^2}\right), \tag{3}$$

where d is the distance of every point along the ray R to the wind turbine, μ takes the zero value so it is centered at the turbine position $wt_{x,y}$, and σ is defined equal to $\max(d)/3$ after a sensitivity analysis (shown in Sect 4.1). Finally, we define $\mathrm{WIX_G}$ as

$$\mathrm{WIX_G} = N_d R. \tag{4}$$

The second version of the WIX takes the wind field climatology statistics W_{wd} to weigh the vector rays depending on the wind direction frequencies f_{wd} at the wind farm location:

$$\mathrm{WIX_C} = \mathrm{WIX_G} W_{wd}, \tag{5}$$

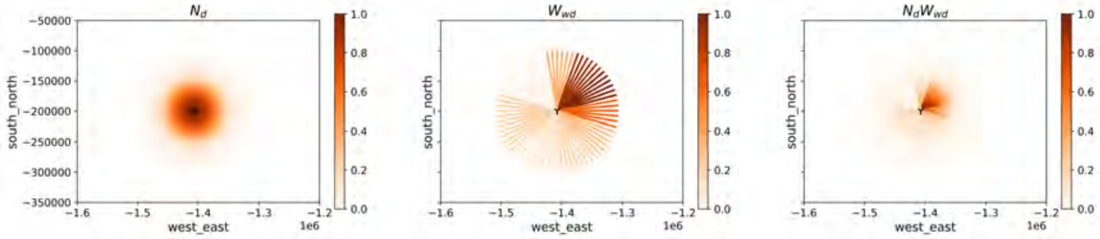

Figure 1: Example of kernels applied to the rays of one turbine. The turbine is located at the center of the circle, and every radial line represents a ray. The left-side panel shows the wake decay kernel N_d, the central panel shows the wind directional kernel W_{wd}, and the right-side panel shows the combination of the two: N_dW_{wd}. The color scale is normalized for the three cases. The map projection is Lambert conformal, and the coordinate units are meters.

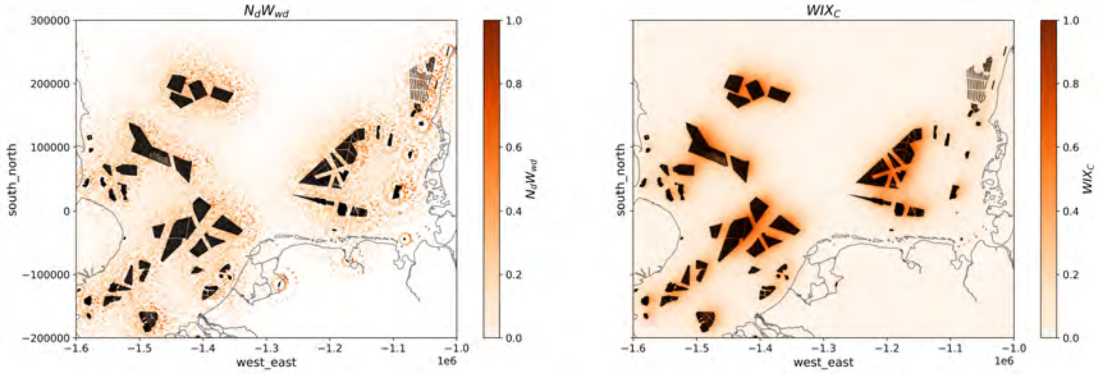

Figure 2: Two stages of the WIX: the left-side panel shows a sample of the ray points colored by the N_dW_{wd} kernel value. The right-side panel shows the next stage after the ray points are computed by the 2D histogram, outputting the WIX. The map projection is Lambert conformal, and the coordinate units are meters.

where

$$W_{wd} = \left(\frac{f_{wd}}{\sum f_{wd}}\right)^2, \tag{6}$$

with the directional kernel W_{wd} (Figure 1-central panel). Finally, the Figure 1-right panel shows the combination of N_dW_{wd}, which is the final kernel applied to the rays.

Once the rays and kernels are defined, a 2D histogram is generated to convert the points and kernel weights into a grid. The 2D histogram calculates the spatial density of points on a defined grid and uses the input kernel N_dW_{wd} to weight such points. Here, we use a grid resolution of 3 km (same as the WRF model grid) in both the x and y directions, consisting of 360 points from south to north and 450 points from west to east. Figure 2 shows the transition from points (left-side panel) to the gridded output (right-side panel).

4 Results

4.1 Sensitivity analysis to the decay factor (σ)

One parameter that requires special attention is the decay factor (σ) from the N_d kernel, as it is crucial for accurately emulating the wake decay with distance, which impacts the final footprint of the index. Hence, a sensitivity analysis was performed by computing the WIX for different decay factors, starting from $\max(d)/1$ to $\max(d)/4.5$ every $\max(d)/0.5$ and comparing the results against the wind speed deficit output from the WRF runs. Figure 3 shows the analysis for the $\mathrm{WIX_C}$ (analysis for $\mathrm{WIX_G}$ not shown), where both versions of the index agree on a sigma equal to $\max(d)/3$ as it provides the higher R^2 value in both cases. Moreover, one can see in Figure 4 how the correlation between datasets peaks at $\sigma = \max(d)/3$ and then drops again, making a selection of the decay factor consistent.

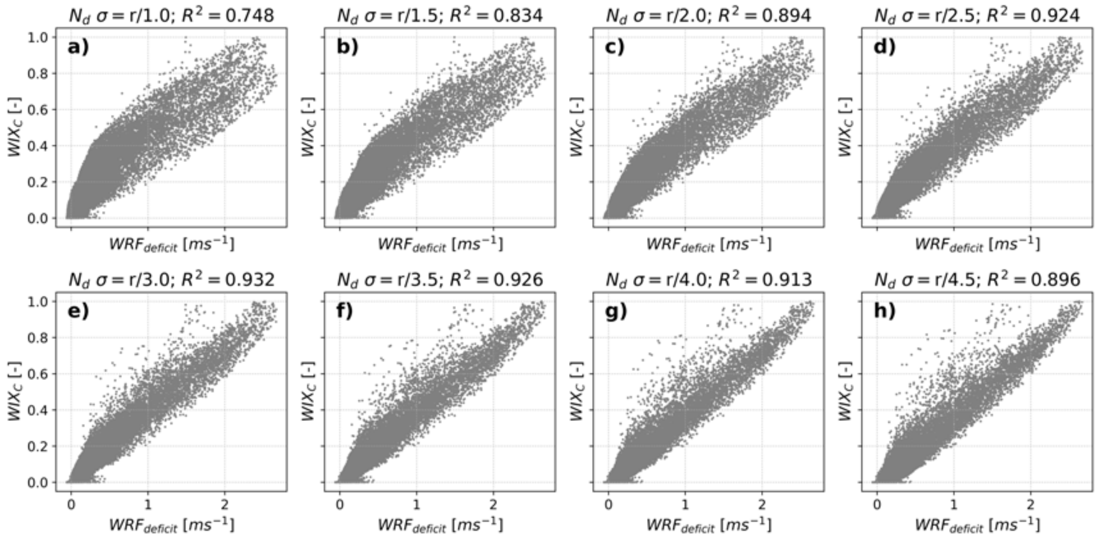

Figure 3: Sensitivity analysis for the sigma decay factor in the N_d kernel. Every panel shows the scatter plot between the $\mathrm{WIX_C}$ and WRF per assessed decay factor. The panels titles show the σ and decay parameter utilized and the R^2 obtained in the comparison.

4.2 Comparison against the WRF model wakes

The results in Figure 5 suggest a good agreement between both versions of the WIX and the WRF model. However, $\mathrm{WIX_G}$ shows stronger differences with respect to WRF, overestimating the upwind areas and generally underestimating the downwind areas. On the other side, $\mathrm{WIX_C}$ shows less differences compared to WRF, agreeing more on the areas where WRF does show wind speed deficits. These differences translates into a linear correlations of 0.88 and 0.93 for $\mathrm{WIX_G}$ and $\mathrm{WIX_C}$, respectively (see the **e** panel in Figure 3 for correlation values). Regarding the computational time, even though both WIX versions show a difference: $\mathrm{WIX_G}$ takes around 15 s, and $\mathrm{WIX_C}$ takes 420 s to run on 32 cores, this is still significantly less than the computation time and resources required for a WRF model simulation to capture the climatology behavior over a representative year. The one shown in this study is between 3 and 17 days, depending on the availability of computational resources, which are required to be 160 cores for 53 runs, lasting 8 hours per run.

5 Discussion and Conclusion

In this study, we demonstrate the effectiveness of the WIX for scenario planning in high-density offshore wind developments. By comparing the geometric variant $\mathrm{WIX_G}$ and the climatological variant $\mathrm{WIX_C}$ against data from the WRF model simulations, we have shown that both WIX approaches can capture regional offshore wind farm wake footprints with sufficient accuracy to

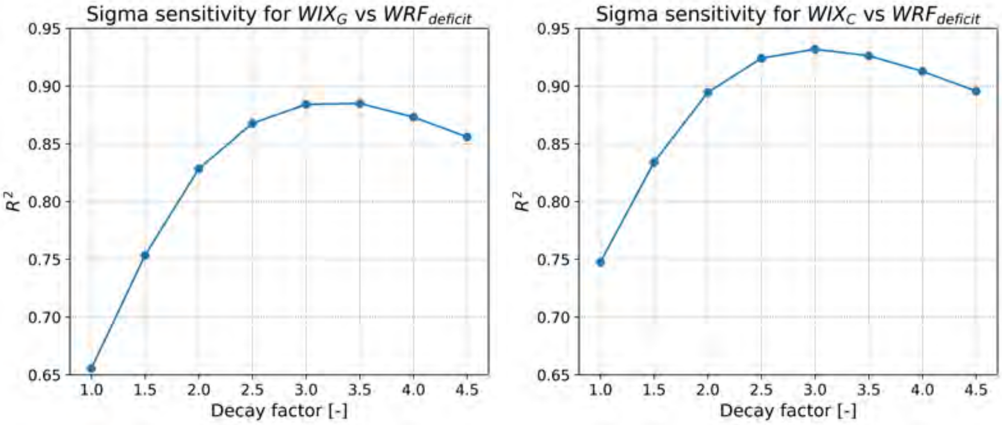

Figure 4: Sensitivity analysis for the sigma decay factor in the N_d kernel. The curves show the R^2 between the WIX and WRF per decay factor number. The left-side panel shows the analysis for the WIX_G, and the right-side panel shows the results for the WIX_C.

inform large-scale preliminary planning decisions. One of the central aims was to address the need for scenario-based workflows in the offshore wind sector, where multiple site layouts must be rapidly evaluated. Given that high-resolution numerical modeling with the WRF model can be computationally and time expensive, the WIX offers a streamlined approach that saves time without sacrificing critical insight before the final spatial assessments.

The WIX has gained interest from governmental agencies and industry consortia, most notably the Danish Energy Agency, which is considering integrating it into future wind energy screening projects. This level of engagement underscores the tool's move from theoretical research toward practical application, signaling its value for large-scale regional planning. It is important to note, however, that neither the WRF model nor the WIX—whether WIX_G or WIX_C—are suited for detailed modeling of wakes within wind farms (and probably also inaccurate for external wakes in many flow conditions). Instead, these tools best serve regional-scale analyses, complementing more advanced microscale models such as LES, CFD, or linearized wake models.

A key finding of this work lies in understanding the trade-off between WIX_G and WIX_C. While WIX_G offers faster run times—essential for screening multiple layout scenarios in rapid succession—WIX_C provides better guidance for wind farm screening at the cost of a longer computation time, roughly twenty-eight times that of WIX_G. This distinction allows stakeholders to select the variant most suitable for their needs, depending on whether broad planning or high-precision analysis is the priority.

Overall, the ability to quickly test numerous wind farm scenarios during the regional planning stage is essential for meeting renewable energy targets while minimizing environmental impacts. The WIX contributes to more efficient and responsible offshore wind development. Looking ahead, the continued integration of tools like the WIX into sustainability and planning frameworks can help optimize large-scale offshore wind projects, balancing the urgency of energy demands with the need to maintain marine environmental integrity.

6 Acknowledgments

We acknowledge the Independent Research Fund Denmark funding through the Multi-scale Atmospheric Modeling Above the Seas (MAMAS) project (no. 0217-00055B) and the EU Horizon Europe project WIMBY (Grant Agreement No. 101083460).

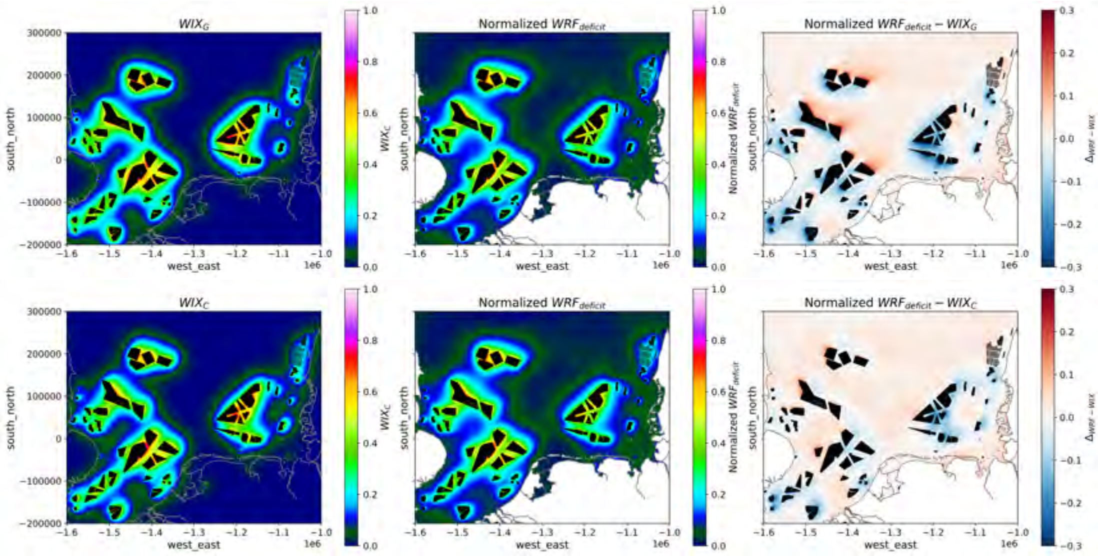

Figure 5: Comparison between the WIX and the normalized WRF-simulated wind speed deficit. The upper row corresponds to $\mathrm{WIX_G}$ and the lower row to $\mathrm{WIX_C}$, both shown on the left-side panel. The central panel corresponds to the WRF model and is identical in both rows. The map projection is Lambert conformal, and the coordinate units are meters.

References

[1] Naveed Akhtar et al. "Accelerating deployment of offshore wind energy alter wind climate and reduce future power generation potentials". In: *Scientific Reports* 11.1 (2021), pp. 1–12. DOI: `10.1038/s41598-021-91283-3`.

[2] R Borgers et al. "Mesoscale modelling of North Sea wind resources with COSMO-CLM: model evaluation and impact assessment of future wind farm characteristics on cluster-scale wake losses". In: *Wind Energy Science* 9 (3 2024), pp. 697–719. DOI: `10.5194/wes-9-697-2024`. URL: `https://wes.copernicus.org/articles/9/697/2024/`.

[3] Bundesnetzagentur. *Marktstammdatenregister (MaStR)*. URL: `https://www.marktstammdatenregister.de/MaStR/Einheit/Einheiten/OeffentlicheEinheitenuebersicht` (visited on 10/19/2021).

[4] M. Dörenkämper et al. "The Making of the New European Wind Atlas – Part 2: Production and evaluation". In: *Geoscientific Model Development* 13.10 (2020), pp. 5079–5102. DOI: `10.5194/gmd-13-5079-2020`. URL: `https://gmd.copernicus.org/articles/13/5079/2020/`.

[5] Energimyndigheten. *Vindbrukskollen – Energimyndigheten, Sweden*. URL: `https://vbk.lansstyrelsen.se` (visited on 09/16/2024).

[6] Energistyrelsen. *Stamdataregisteret for vindkraftanlæg*. URL: `https://ens.dk/service/statistik-data-noegletal-og-kort/data-oversigt-over-energisektoren` (visited on 10/20/2021).

[7] European Marine Observation and Data Network (EMODnet). URL: `https://emodnet.ec.europa.eu/en/human-activities` (visited on 01/02/2022).

[8] Jana Fischereit, Marc Imberger, and Xiaoli Guo Larsén. "Cost-effective mesoscale modeling methods for offshore wind resource assessment with farm wake effect". English. In: *WindEurope Technology Workshop 2022 : Resource Assessment and Analysis of Operating Wind Farms*. 2022. URL: https://windeurope.org/tech2022/.

[9] Anna C. Fitch et al. "Local and Mesoscale Impacts of Wind Farms as Parameterized in a Mesoscale NWP Model". In: *Monthly Weather Review* 140.9 (2012), pp. 3017–3038. DOI: 10.1175/MWR-D-11-00352.1. URL: https://journals.ametsoc.org/view/journals/mwre/140/9/mwr-d-11-00352.1.xml.

[10] Evan Gaertner et al. *Definition of the IEA 15-Megawatt Offshore Reference Wind Turbine*. Tech. rep. International Energy Agency, 2020. URL: https://www.nrel.gov/docs/fy20osti/75698.pdf.

[11] O. García-Santiago et al. "Evaluation of wind farm parameterizations in the WRF model under different atmospheric stability conditions with high-resolution wake simulations". In: *wes* 9 (2024), pp. 963–979.

[12] Oliver Maas and Siegfried Raasch. "Wake properties and power output of very large wind farms for different meteorological conditions and turbine spacings: a large-eddy simulation case study for the German Bight". In: *Wind Energy Science* 7 (2 Mar. 2022), pp. 715–739. ISSN: 2366-7451. DOI: 10.5194/wes-7-715-2022.

[13] OpenStreetMap contributors. *Planet dump retrieved from https://planet.osm.org*. https://www.openstreetmap.org. 2021. (Visited on 01/10/2022).

[14] A. Peña, J. D. Mirocha, and M. P. van der Laan. "Evaluation of the Fitch wind-farm wake parametrization with large-eddy simulations of wakes using the Weather Research and Forecasing model". In: *mwr* 150 (2022), pp. 3051–3064.

[15] The Wind Power. *Europe wind farms database*. URL: https://www.thewindpower.net/store_continent_en.php?id_zone=1001 (visited on 01/10/2021).

[16] P J H Volker et al. "The Explicit Wake Parametrisation V1.0: a wind farm parametrisation in the mesoscale model WRF". In: *Geoscientific Model Development* 8 (11 2015), pp. 3715–3731. DOI: 10.5194/gmd-8-3715-2015. URL: https://gmd.copernicus.org/articles/8/3715/2015/.